IMPACT OF INSERTION LOCATION ON THE LONGEVITY OF A MARS BALLOON

Scot C. R. Rafkin

Southwest Research Institute, Dept. of Space Studies, 1050 Walnut St., Suite 300, Boulder, CO, USA, 80302
rafkin@boulder.swri.edu

ABSTRACT

Mars is considered a planet where balloon exploration is feasible. Due to the relatively thin atmosphere, however, balloons generally need to fly at low altitudes. This presents a problem, because Mars has extreme topography, a good portion of which is not navigable by a balloon. Using output from GCM and mesoscale models, we show that a careful choice of probe insertion location can maximize the longevity of a superpressure (constant density) balloon. At the same time, improper selection can result in a very short mission lifetime.

1. INTRODUCTION

Trajectory analyses of a constant-density, superpressure balloon are performed at a variety of density altitudes near L_s=165. Knowledge of balloon flight path will be critical to establishing the probability of achieving science goals. Balloons that impact the elevated surfaces of Mars in a short period of time will prematurely terminate science return and could fail to achieve floor longevity requirements.

The methodology used to establish trajectories is first described. Then, the results from trajectory analyses computed at Ls=165 (which corresponds to the most energetically favorable orbit transfer in the 2013 launch window) are presented.

2. METHODOLOGY

2.1 Displacement Equation

The balloon trajectory is computed by integrating the balloon velocity with respect to time to obtain displacement:

$$\left| \vec{r} = \int_{t'}^{t'+\Delta t'} \vec{V}(x,y,t)dt \right|_{\rho} , \qquad (1)$$

where $\vec{r}$ is the position vector, and $\vec{V}$ is the horizontal balloon velocity. A super-pressure balloon flies along an isopycnal (constant density) surface, and thus Eq. (1) is evaluated on a specified constant density surface.

The balloon velocity is taken to be equivalent to the atmospheric velocity. The validity of this assumption is evaluated by considering the horizontal equation of motion for the balloon and the atmosphere:

$$\frac{d\vec{V}}{dt} = -f\hat{k} \times \vec{V} + \frac{1}{\rho_a}\nabla p + \frac{\vec{V} - \vec{V}_a}{\tau} \quad , \qquad (2)$$

where f is the coriolis parameter, p is the atmospheric pressure, subscript a refers to the atmosphere, and the dynamic force on the balloon is modeled by the last term of Eq. (2) using an adjustment time scale of τ. The adjustment time scale is on the order of a minute, and represents the characteristic time it takes for the balloon to attain a speed of 1 m/s when starting from rest in an atmosphere moving at 1 m/s. Note that the density of the balloon is taken as the density of the atmosphere by definition for a neutrally buoyant system.

An order of magnitude analysis of the accelerations in Eq (2) are in order. If the balloon speed is different than the wind speed by 1 m/s, the acceleration due to the last term is on the order of 0.01 ms^{-2}. In the subtropics, where gradient wind dominates, the first two terms on the r.h.s of Eq. (2) are nearly in balance, with a typical residual of less than 10%. Using a typical winds speed of 20 m/s and latitude of 45°, the coriolis term produces an acceleration of order $5x10^{-5}$. Therefore, the last term in Eq. (2) is orders of magnitude larger than the other accelerations and their residuals. In short, the balloon will very quickly adjust to the atmospheric velocity when outside the tropics.

Within the tropics, the coriolis torque is negligible. In the atmosphere, the winds in the tropics are dominated by irrotational motions that develop in response to the pressure gradient. On the large-scale, some of the strongest horizontal pressure gradients in the Martian tropics result from the thermal tide. On smaller scales, thermal circulations resulting from topography can also produce strong pressure gradients. A pressure gradient of order 1000 Pa/km (assuming an atmospheric density of order 10^{-2} kg m^{-3} would be required to rival the adjustment acceleration, which is not realistic. Therefore, even in the tropics, the balloon will adjust

very quickly to the atmospheric wind regardless of the other forces, and the assumption that the balloon velocity is equivalent to the wind velocity is valid as long as the environment wind changes over timescales much more slowly than the adjustment time scale.

In some cases, particularly in the convective and turbulent daytime planetary boundary layer (PBL), it is possible to imagine that the environment velocity would change faster than the balloon could adjust. The proper representation of balloon behavior in this environment would require complex aerodynamic modeling of the balloon, which is beyond the scope of this work. However, in addition to balloon trajectory considerations in such an environment, the possibility for excitement of unwanted pendulum oscillations in the balloon-gondola system are recognized. The Mars Exploration rovers were susceptible to similar oscillations. Any balloon system encountering the Mars PBL should consider the entire range of balloon system behavior.

2.2 General Circulation Model Description

Having shown that the balloon velocity may be taken as the atmospheric velocity in most cases, the integration of Eq. (1) still requires knowledge of the winds. The atmospheric state is taken from a simulation conducted with the Ames Mars General Circulation Model (MGCM) version 1.7.3. The particular simulation uses a 5x6 degree latitude by longitude domain and is forced by a variable dust opacity description. Dust is varied in time and latitude in such a way that it matches the zonally averaged dust opacity retrieved by the Thermal Emission Spectrometer in Mars Global Surveyor mapping year one.

Topography is derived from Mars Orbiter Laser Altimeter (MOLA) data re-binned to 5x6 degrees and filtered with a 9-point smoother. As shown in Fig. 1, the model captures the essence of the true Mars topography, although the high montes of Tharsis and elsewhere are understated, and the Tharsis plateau is generally broader and higher than reality. The height of the Tharsis bulge in the MGCM is, therefore, a conservative lower boundary. The highest peaks are not of concern for this particular study since the balloon altitudes under consideration are much lower; the balloon would impact the surrounding plains and slopes before it hit the peaks.

2.3 Flight Level Winds

The pressure cycle from the MGCM was compared to the Viking Lander pressure timeseries to determine how accurately the model was in reproducing the mass cycle. This is important because the MGCM data, which is natively on sigma-pressure surfaces must be interpolated to a constant density surface. Errors in the model pressure will lead to errors in density, and the true height of a density surface above the ground level will be in error.

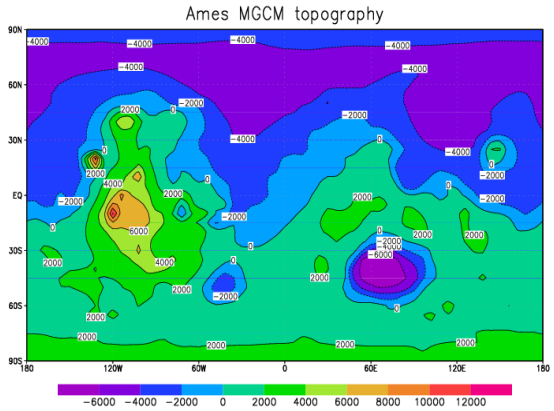

Figure 1. Topography in the 5x6^{o} Ames MGCM simulation used for the trajectory calculations. All the large, major topographic barriers are resolved. However, the montes peaks are less than half their true height, and the Tharsis plateau is broader and slightly higher than that of Mars. Still, the peaks are higher the balloon altitudes considered and the broad, high plateau provides a conservative assessment for topographic impact.

The MGCM data was interpolated to the lander locations and then hydrostatically reduced to the correct altitude using the average diurnal temperature in the lowest 10 km to compute the scale height. The model was anywhere from 2-4% to high depending on season and location. That the model offset is not uniform for VL1 and VL2 for a given season and this is indication of intrinsic model error rather than an initial incorrect specification of total CO_2 in the system.

To remove as much of the systematic model error as possible from our calculations, the model densities and pressures are scaled so as to minimize the offset between the model and the observed pressure cycles. The scaling factor is a few percent at most. We note that even after the scaling, the pressure cycles are typically off by ~1%, as it is not possible to produce simultaneous agreement between the model and both observation locations.

After scaling, it is prudent to recognize that the model values are still likely to be off by several percent or more compared to the Mars atmosphere at the time of balloon insertion and flight. Small changes in atmospheric dust loading produce relatively large

changes in the density profile, and such changes in dust loading are stochastic.

Notwithstanding the scaling, two locations in the northern hemisphere are not nearly enough to adequately establish the global pressure cycle. A statistically significant number of stations (*i.e.*, a number much greater than two) are required to make a more meaningful model correction. However, there are only two stations available, and we make use of what is available.

After adjusting the model based on the Viking Lander pressure data, the model fields are interpolated to a constant density surface. An isopycnal surface must be selected on which to integrate Eq. (1). This is done by selecting a starting Ls and desired balloon altitude. The average global density at that altitude is computed from the GCM output averaged over a 30 sol time period beginning with the selected starting Ls. Of course, the actual height of any given density surface will vary in time and space, but the above described mention guarantees that on a global and time average, the density surface is at the desired altitude. The results of this calculation for a variety of float altitudes is shown in Table 1. Locations where the isopycnal surface intersects or is below the topography are flagged and stored for use during the trajectory calculations.

Table 1. Global Average Density (kg/m^3)

Ls	z=0 km	z=2km
135	.01245	.01111
140	.01245	.01104
145	.01247	.01100
150	.01250	.01110
155	.01260	.01102
160	.01270	.01108
165	.01290	.01115
170	.01305	.01123
175	.01327	.01133
180	.01350	.01146

2.4 Trajectory Integrations

Eq. (1) is solved numerically through discretization:

$$\Delta\vec{r} = \vec{V}_h(x,y,t)\Delta t \ . \qquad (2)$$

The velocity is obtained by interpolating the GCM output in time and space. A six minute time step (Δt) is used in the integration. After each time step, the computed change in the position vector is decomposed into a bearing and distance, which is then used along with the previous position to obtain the new location. From spherical trigonometry, it can be shown that given an original latitude/longitude position (φ_1, λ_1) and a bearing θ and distance *d*, with planetary radius, *R*, the new latitude/longitude position (φ_2, λ_2) is given by

$$\varphi_2 = \sin^{-1}(\sin\varphi_1 \cos\frac{d}{R} + \cos\varphi_1 \sin\frac{d}{R})\cos\theta, \qquad (3)$$

and

$$\lambda_2 = a\tan2(\sin\theta \sin\frac{d}{R} + \cos\varphi_1 \cos\frac{d}{R} - \sin\varphi_1 \sin\varphi_2)\cdot \qquad (4)$$

In practice, the balloon trajectory calculations involve a number of steps. First, the average density of a specified altitude is calculated over a 30 sol window beginning at a given Ls (*cf.* Table 1). The result is used to interpolate the meteorological data from each GCM output time (ever 1.5 Mars hours) to the specified isopycnal surface.

Integration requires two initial conditions: the starting time and the starting location. For these studies, a local time of 1400 is selected for no other reasons than: 1) it makes sense to deploy during the day when the sun is up and power is immediately available; and 2) this roughly when the MERs landed. In reality, the actual landing time will depend on many factors, including the requirement for direct-to-Earth communication during critical entry, descent, and inflation sequencing. The initial starting location depends on the trajectory

After specifying the initial conditions, the isopycnal data (previously interpolated from the full GCM output) are further interpolated in space and time to the balloon location. The interpolation in space uses a weighting scheme inversely proportional to distance. So, model grid point locations closest to the balloon location are given the most weight. Time interpolation is linear between GCM output times. The GCM fields are then once again interpolated in space and time to obtain values at a Δt time later, but at the same initial balloon location. Thus, there are now two sets of balloon data, those valid at the initial time at the initial balloon location, and those valid at a small time increment later also at the initial balloon location.

Next, the zonal (*u*) and meridional (*v*) components of the wind for the two balloon times are individually averaged to produce a single, average wind vector $(\bar{u}, \bar{v})$ valid over the time interval Δt. It is these values that are used in Eq. (2), which is split into component form:

$$x_{t+\Delta t} = x_t + \bar{u}(t, t+\Delta t)\Delta t, \qquad (5)$$

and,

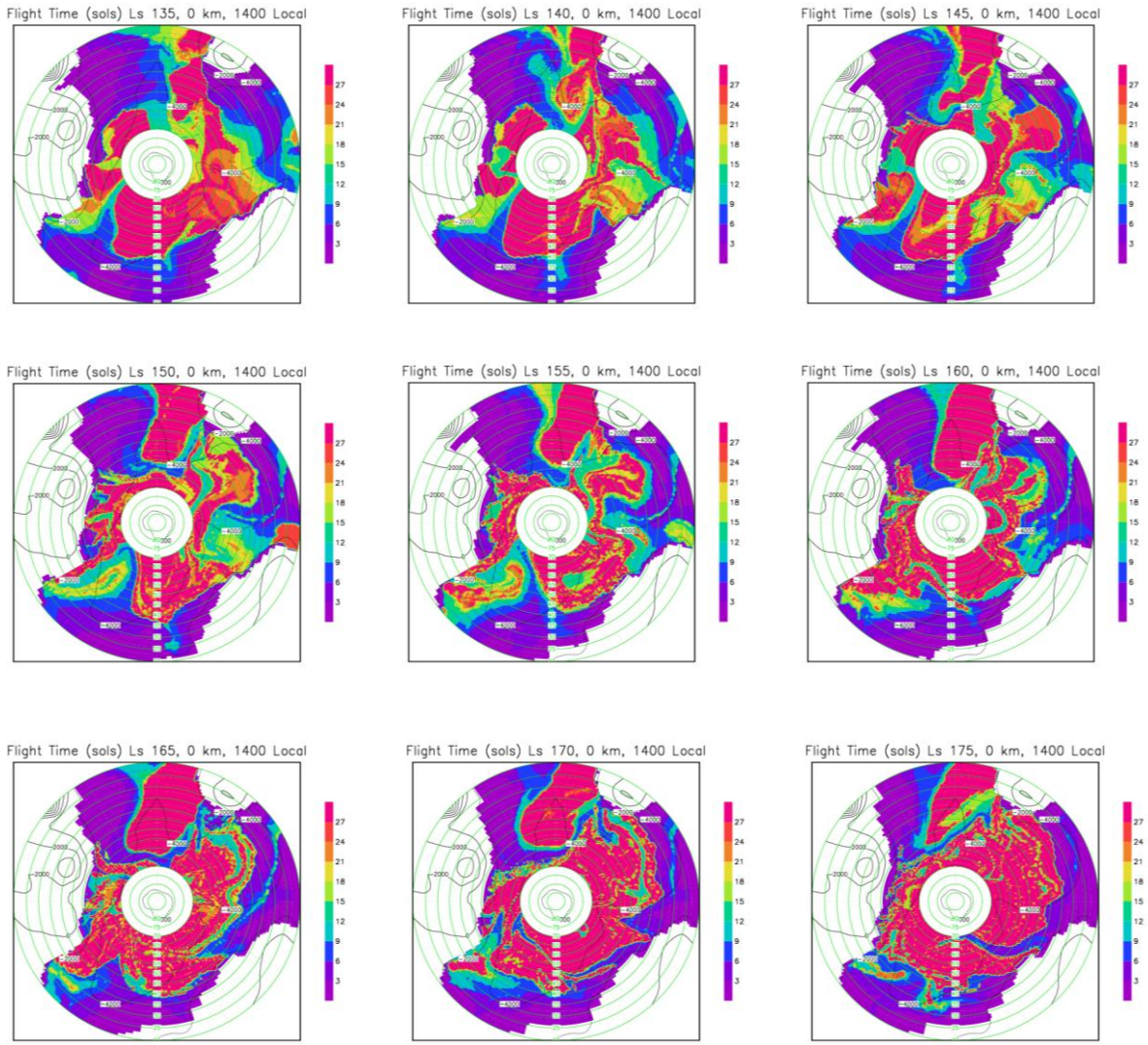

Fig. 2. Flight time for a balloon launched from a given location for different starting Ls. Unshaded areas indicate regions where 0 km MOLA is below ground.

$$y_{t+\Delta t} = y_t + \bar{v}(t, t+\Delta t)\Delta t. \qquad (6)$$

The new balloon positions given by Eqs. (5)-(6) are then converted to a distance and bearing from the starting location, and these are then substituted into Eqs (3)-(4), to give provide the latitude/longitude location of the balloon at time $t+\Delta t$. The procedure of spatial and temporal resolution is then repeated to step the balloon location forward to time $t+2\Delta t$.

In some cases, the isopycnal surface will intersect the ground. When this happens, any data points below the ground are not used in the trajectory calculations (*i.e.*, the weights of these points in the spatial averaging are set to zero). The balloon is assumed to experience unplanned ground sampling event (*i.e.*, it crashes), if the altitude of the balloon is found to be below the GCM topography that has been spatially interpolated to the balloon location. Typically, if the balloon is still flying after approximately 30 sols of integration, the simulation is stopped, although the time cut-off can be changed as needed.

During the balloon integration, environmental values (temperature, pressure, winds) and location (including local topography elevation) are stored in an output file at 1 hour intervals. These data are then used to analyze the flight paths, as described in the next section.

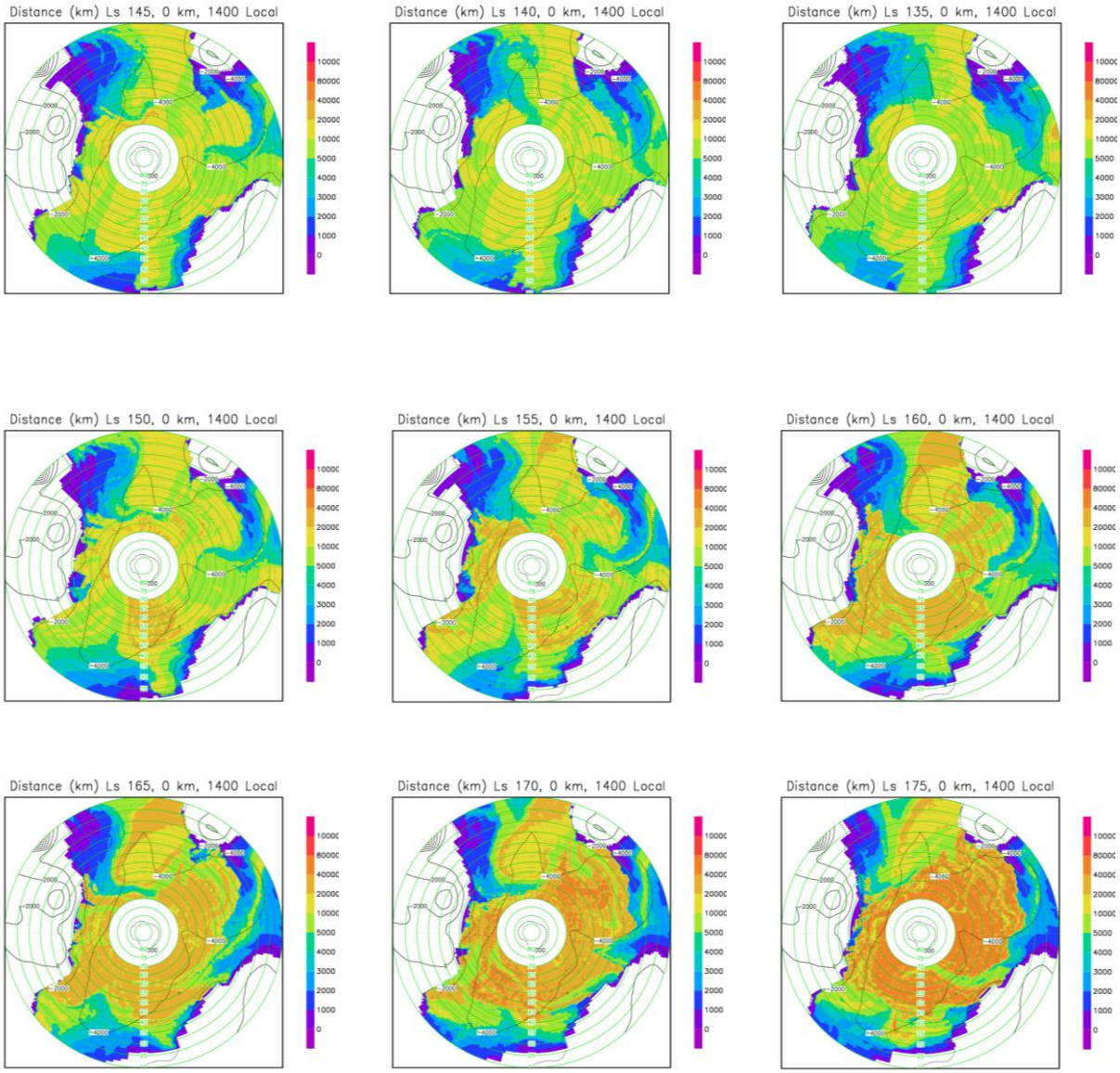

Fig 3. Same as Fig. 2, but for distance.

There are two basic types of trajectory calculations. In the first, the planet is divided into a 2x2 degree grid, and balloons are launched from each location. Statistics from each of these balloon flights are calculated and used to produce contour maps. Examples of statistics and maps include time of flight, distance traveled, average speed, maximum speed, average height above ground level, *etc.*

The second type of trajectory calculation investigates the solution stability of launching from a particular location. This scenario involves perturbing the initial launch location of the balloon by fractions of a degree to provide initial launch locations for additional trajectory calculations. The trajectory of the balloons are plotted on the same map to provide so-called "spaghetti plots". If the solution is stable, each of the initial perturbations will result in trajectories that overly one another. Often, the trajectories display chaos, with a preference for trajectories to cluster around two or more possibilities. This second type of trajectory calculation is too computationally expensive to be done for each 2x2 degree grid point. Therefore, the globally gridded trajectory results are inspected and solution stability calculations are initiated based on launch locations that look interesting.

3. RESULTS

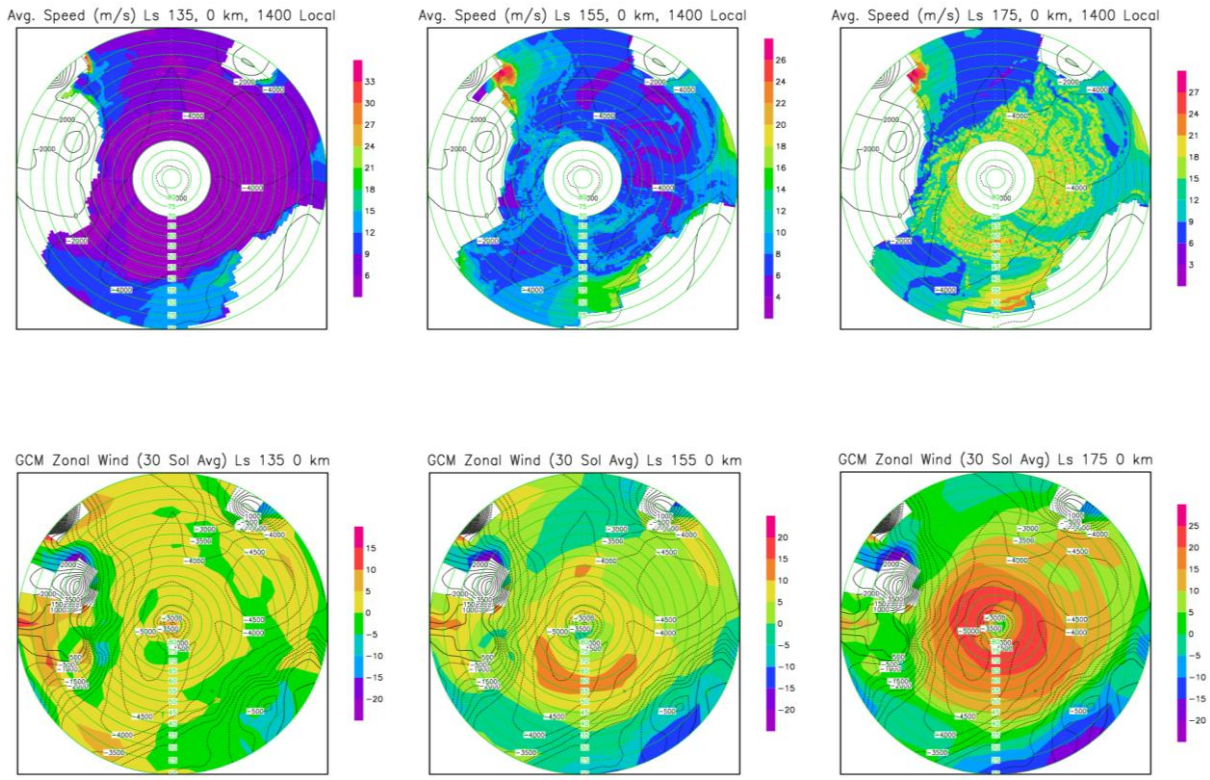

Fig 4. Same as Fig. 2, but for average balloon speed (top row). Bottom row shows mean zonal wind from the GCM.

Fig. 2 shows the flight duration for a balloon launched from a given duration as a function of Ls at a target density altitude of 0 km MOLA. Areas shaded in red indicate launch locations that satisfy a nominal 30 sol mission duration requirement.

At all seasons there are broad regions of potential locations that meet the 30 sol requirement. In general, the most favorable locations are on the northern plains between Tharsis and Syrtis Major. At early Ls, there is a broad, solid region of favorable locations in Acidalia Planitia (~0°W). Over time, this area retreats northward, narrows, and generally becomes pockmarked with a few duration times below 30 sols. Another region, just to the east of Elysium Mons in Arcadia Planitia (~170°E) becomes increasingly favorable with time up through about Ls=165. Later in the season, Utopia Planitia (~70°W) becomes increasingly favorable. There is some time of day dependence to the trajectory solutions, but the overall patterns are quite stable regardless of launch season.

The distance travelled by the balloons is shown in Fig. 3. There is a clear correlation between flight time and distance travelled. So, in general, the longer the balloon stays aloft, the greater distance it will travel. There is also a clear trend for the distance traveled to increase as a function of Ls. As reference, consider that with a radius of ~3.39x10^3 km, a circumnavigation at 60° latitude corresponds to ~11,000 km. Thus, at the earlier seasons, most balloons would fall short of circumnavigation at this latitude in 30 sols, and this does not take into account that the balloon trajectories are often sinuous. **Broadly speaking, while all Ls provide large launch regions of satisfactory duration, only the in the later season are travel distances sufficient to allow the possibility of circumnavigation within 30 sols.**

The increasing travel distance as a function of Ls is consistent with the gradual strengthening of the polar jet; the balloons experience a stronger zonal wind, on average (Fig. 4 shows average speed). The increase of patchiness of the time travel field within otherwise large expanses of flight times as a function of Ls is also consistent with the increasing speed and distance travelled. Quite simply, the farther the balloon travels, the more likely it is to run into trouble. Balloons move around the polar vortex, and occasionally they will drift a bit too far south and impact the higher topography. This is mostly a random event as evidenced by the relatively uniform distribution of shorter flight times spread throughout the 30 sol flight time field. **As such, balloon trajectories are not deterministic. At best, only a probability of**

achieving a 30 sol flight time can be established for a balloon launched in a given region.

Table 2. Percentage of Balloons Surviving for 30 Sols

Ls	Latitude range	Longitude range	30-sol Survival %
135	45-60N	0-20W	99.2
145	45-50N	0-10W	100
135	40-50N	150-165E	100
145	20-30N	160-170E	100
160	50-60N	25-25E	94
170	50-60N	10-40E	99.1

Table 2. shows the percentage of balloons that achieve a 30 sol flight time within various specified launch regions and times. This information is most useful for considering the probability of achieving a 30 sol flight time when considering both ground impacts and available power. The launch location windows in Table 2 are not meant to fully cover all the suitable launch times and regions. **Rather, the data show that there are suitable launch regions available over all Ls.**

Balloons launched prior to ~Ls 165 do not run the risk of encountering the polar night until after the 30 sol primary mission. Therefore, minimum floor survivability is approximately 12 hours of darkness and cold. Balloons arriving after Ls 165 do run the risk of encountering extended periods of darkness. Using a launch time of Ls=180 in the area 50-60N and 10-40E, and assuming total darkness above 82N, only two balloons out of 52 were found to exceed 24 hours of darkness. This does not include the possibility of an additional ~12 hours of darkness following emergence from the polar night. None were found to go in

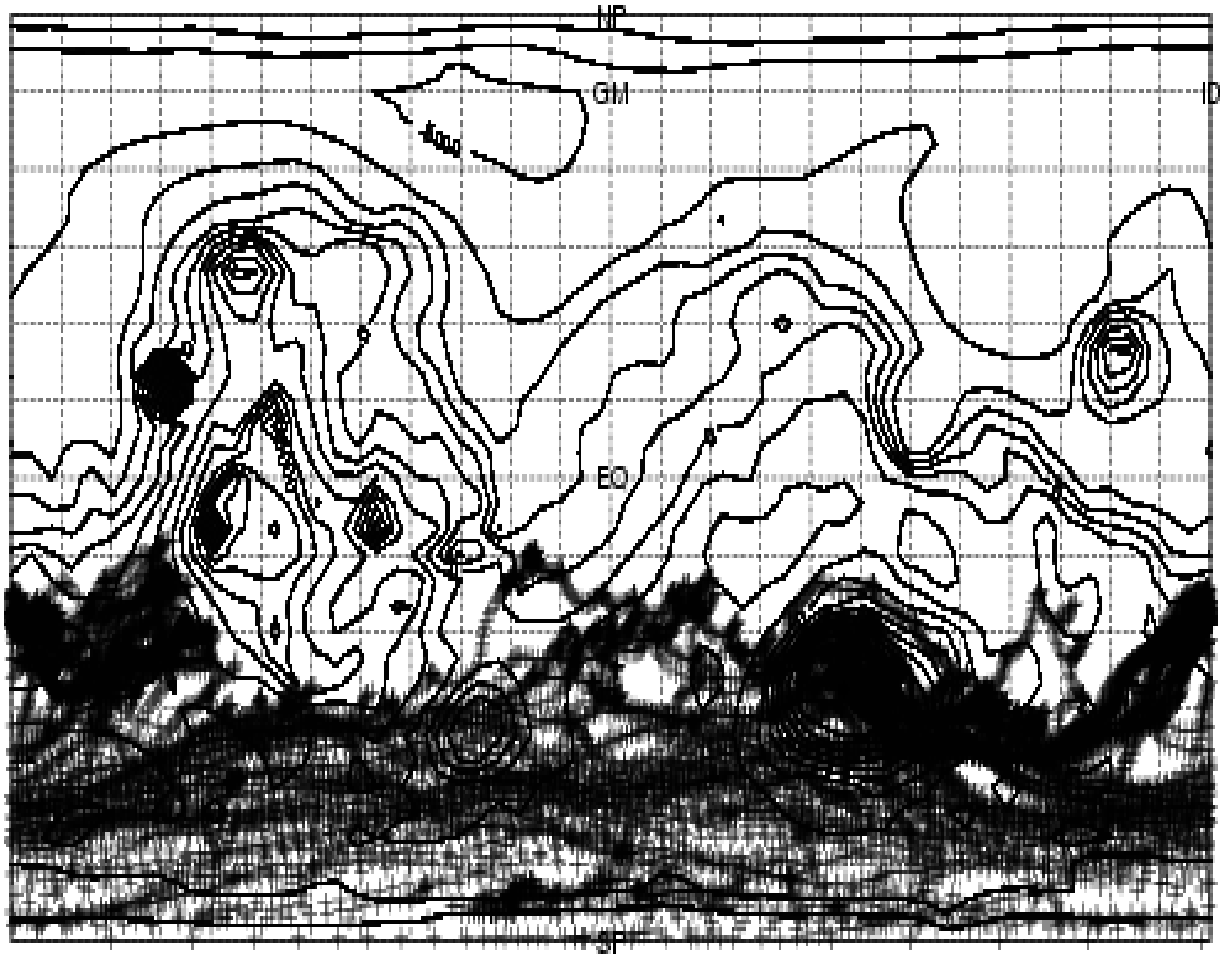

Figure 5. Spaghetti plot for a balloon launch centered in Hellas (42S, 70E). Trajectories are calculated with 0.2° offsets from this location extending 0.5° from the center. The probability of following a particular trajectory is proportional to the density of the trajectories. Two solutions are most probable: one leaves Hellas and then turns northeast toward Tharsis where it terminates; the other goes poleward and completes numerous high latitude circumnavigations. Tick marks are plotted every 1.5 mars hours

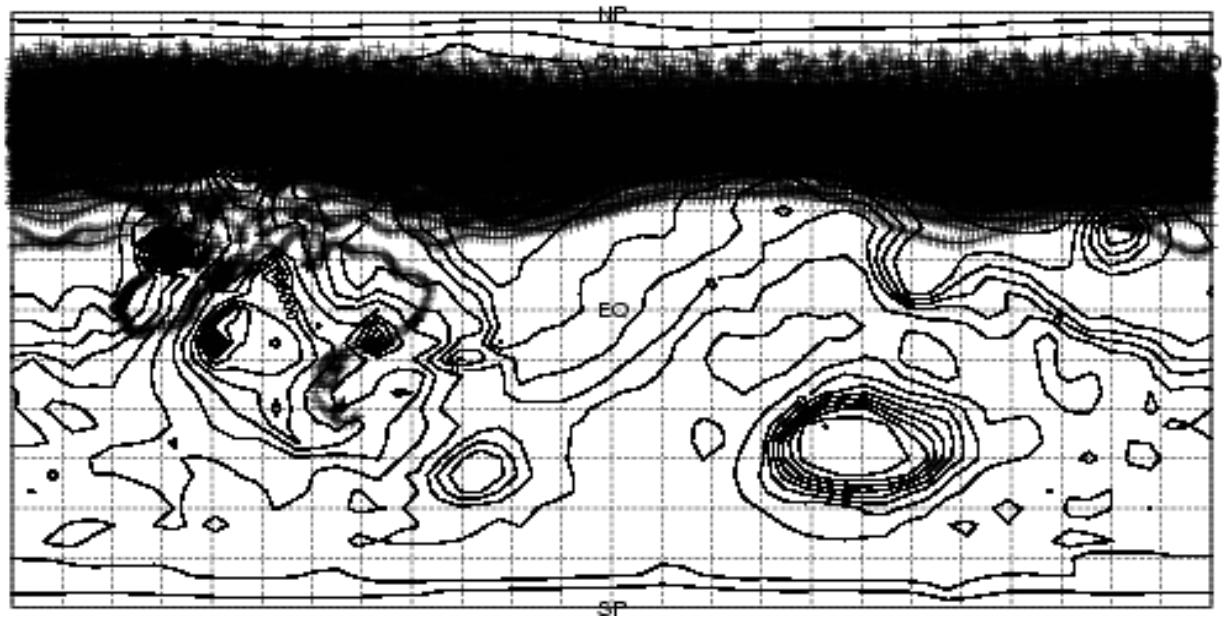

Figure 6. Spaghetti plot for launches centered in Acidalia Planitia (45N, 30W). The dominant solution are subtropicl to high latitude circumnavigations. One minor solution results in balloon flights terminating in the Tharsis region. The density of the circumnavigation trajectories indicates that all paths are roughly equally probable. However, the sharp gradients at the circumnavigation boundaries indicates that the latitude range is strongly constrained

darkness longer than 72 hours. However, this number would clearly change if the latitude of the polar night were changed. Thus, the probability of exceeding 24 hours of darkness is given by p=2/52 (=4%) for a single randomly selected flight, and p=1/52 (=2%) for darkness beyond 27 hours. Also bear in mind the statistics of small numbers; the histogram is not well populated for long durations of darkness.

Spaghetti plots were generated for balloons launches centered in Hellas (42S, 70E), Acidalia Planitia (45N, 30W), and northwest of Terra Merdiani (0N, 10W). These locations show moderate to long flight times. In each case, trial balloons are launched from locations corresponding to points on a grid centered at the points indicated above and which extend 0.5 degrees in either direction at intervals of 0.2 degrees.

There are two dominant trajectory regimes in the Hellas launch (Fig. 5). The first is short distance flights that briefly move southeast out of Hellas but then turn to the northeast where they terminate at Hellas. The second regime turns southeast out of Hellas and then circumnavigates the planet at high latitude. The density of the trajectories is proportional the probability of following a particular trajectory. The trajectories terminating at Tharsis are clustered fairly tightly, indicating that once on that path, the balloon location and fate is relatively deterministic. In contrast, the circumnavigation solutions are not nearly as dense. Some circumnavigation paths are near the pole while others are at 60°. In addition to the two dominant solutions, there are also a few other minor possibilities, which include deviations into the Terra Meridiani region.

The launches within Acidalia (Fig. 6) exhibit entirely different characteristics than those from within Hellas. There is only one dominate solution, which is subtropical to high latitude circumnavigation. The density of the trajectories is large and uniform in a belt from about 30N to 75N, indicating no particular preference for any latitude within this belt. However, the gradient drops off sharply on at the edge of the latitude belt. One minor, but poorly clustered solution results in flights that terminate in the Tharsis region.

Launches from Terra Meridiani (Fig. 7) are indicative off a gauntlet of sorts. Nearly all the balloons meander in the launch region before ejecting toward the northwest rim of Hellas. A substantial fraction of the balloons meet their fate on the rim. A few divert around the north rim of Hellas. Some of these drift toward an eventual impact with Tharsis, and few deflect southward around Tharsis where they

circumnavigate at high souther latitudes. Some of the balloons deflect southward around Hellas, avoiding Tharsis altogether and enter the circumnavigation trajectories.

An additional feature of note for slow moving balloons is the cycloid motion, which is most apparent for the balloons moving north of Hellas. One cycloid is completed each sol, which is highly indicative of influence from the thermal tide. An inertial oscillation could also play a role, but is rejected as the cause since the effects would be minimal in the tropical latitudes where cycloid trajectories are present.

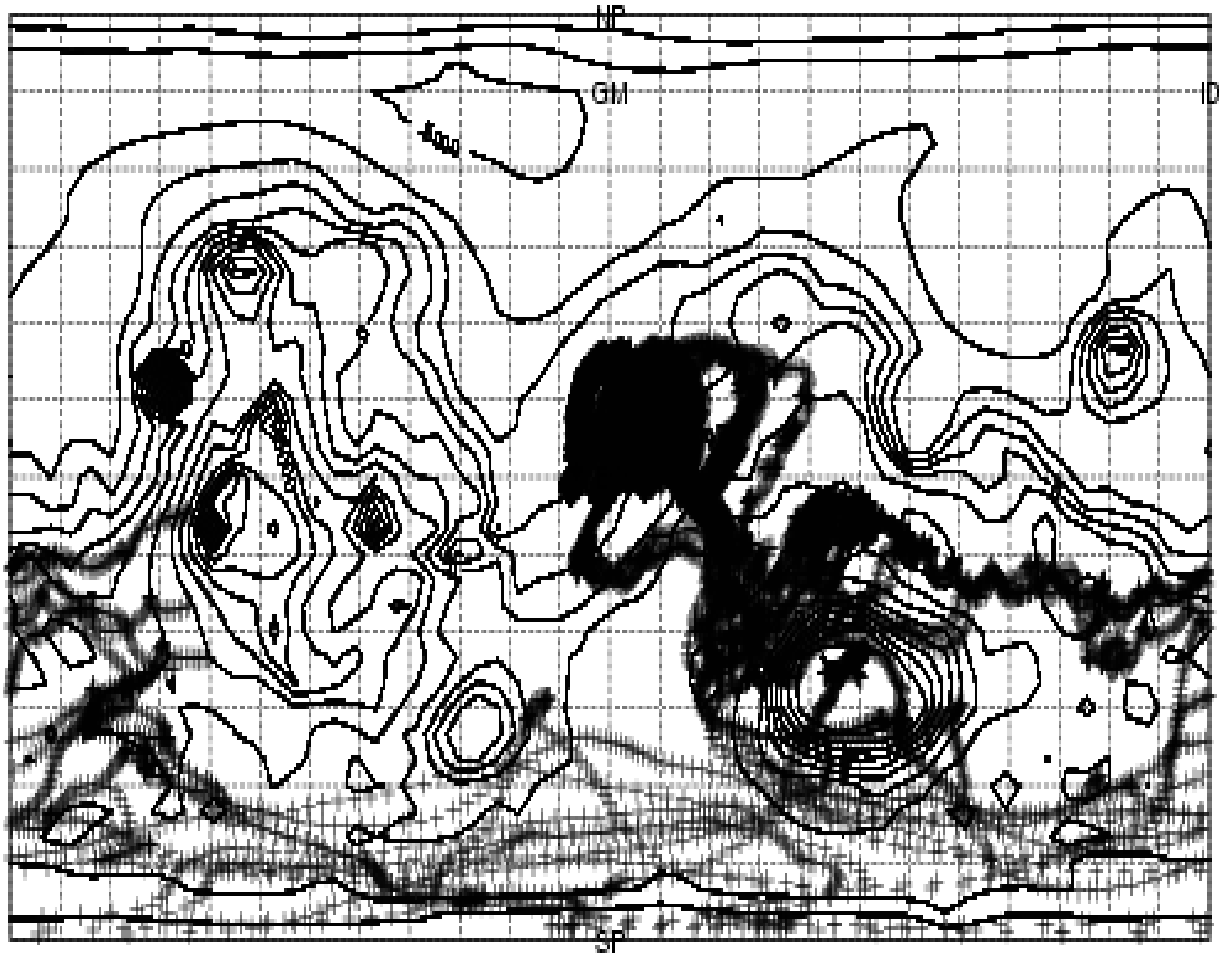

Figure 7. Same as F/ig. 5 but for launches from Terra Meridiani.